Available online at www.sciencedirect.com
ScienceDirect
Materials Letters 61 (2007) 3578–3581
materials letters
www.elsevier.com/locate/matlet

Growth and optical properties of ZnO nanorods by introducing ZnO sols prior to hydrothermal process

Yanhong Tong [a,b,c], Lin Dong [d], Yichun Liu [c,*], Dongxu Zhao [a], Jiying Zhang [a], Youming Lu [a], Dezhen Shen [a], Xiwu Fan [a]

[a] Key Laboratory of Excited State Process, Changchun Institute of Optics, Fine Mechanics and Physics, Chinese Academy of Sciences, Changchun 130033, China
[b] Graduate School of Chinese Academy of Sciences, Beijing 100039, China
[c] Center for Advanced Opto-Electronic Functional Material Research, Northeast Normal University, Changchun 130024, China
[d] School of Materials Science and Engineering, Zhengzhou University, Zhengzhou 450052, China

Received 10 May 2006; accepted 26 November 2006
Available online 12 December 2006

Abstract

ZnO nanorods of 25 nm with quite homogeneous size and shape have been fabricated by introducing ZnO sols as nucleation centers prior to the hydrothermal reaction. The samples were characterized by scanning electron microscope, transmission electron microscope, X-ray diffraction, photoluminescence and resonant Raman spectra. After ZnO sols are introduced, the width of the resulting nanorods decreases above an order of magnitude and the aspect ratio increases 5 times. The increase of the intensity ratio of ultraviolet to visible emissions in room-temperature photoluminescence spectrum and the decrease of the Raman linewidths show the improvement in the quality of ZnO nanorods. Influences of the number of seed nuclei and the aging time of ZnO sols on the morphology of ZnO nanorods are discussed.

Keywords: ZnO nanorods; Hydrothermal synthesis; Nucleation centers; Optical properties

1. Introduction

Recently, one-dimensional (1D) ZnO nanostructures have been attracting much attention due to their novel properties and the potential application in optoelectronics and device miniaturization [1,2]. Numerous techniques have been used to fabricate diverse 1D ZnO nanostructures [3–6]. Among them, the simplest and the most economical methods are vapor transport process and hydrothermal technique. Compared with other methods, the hydrothermal technique has many merits such as large-scale manufacture and low synthesis temperature. Therefore, the hydrothermal process has been used quite extensively to fabricate various 1D ZnO nanostructures, including nanorods, nanowires and nanotubes [7–10]. However, the large-size 1D ZnO structures with a width in micron and submicron range are generally obtained and the aspect ratio is low, which makes the quantum confinement effect inappreciable and hinders the application of 1D ZnO nanostructures in nanoscale photonics and electronics. Recently, well arrayed ZnO nanorods with the width of about 50 nm have been obtained by depositing ZnO nanocrystal layers on substrates prior to hydrothermal growth [11]. It is proposed that the ZnO nanocrystals and the interfaces between the nanocrystals provide a large number of nucleus sites which facilitate decreasing the width of ZnO nanorods [12–14]. However, it is difficult to further decrease the width of nanorods, and the obtained nanorods of 50 nm have to be confined to substrates.

In this letter, we introduced excessive small-size ZnO sols as seed crystals prior to the hydrothermal process. The ZnO sols directly act as nucleation centers, and the growth need no longer overcome the nucleation barrier. The existence of a large number of the nucleation centers is expected to make less stock solution consumed at each growth point, resulting in the decrease in the size of ZnO nanorods. Our experimental results show that the width of 1D ZnO nanostructures can be dramatically decreased by introducing ZnO sols and the size of the obtained ZnO nanorods is quite homogeneous. Further,

* Corresponding author. Tel.: +86 431 5099168; fax: +86 431 5684009.
E-mail address: ycliu@nenu.edu.cn (Y. Liu).

0167-577X/$ - see front matter © 2006 Elsevier B.V. All rights reserved.
doi:10.1016/j.matlet.2006.11.125

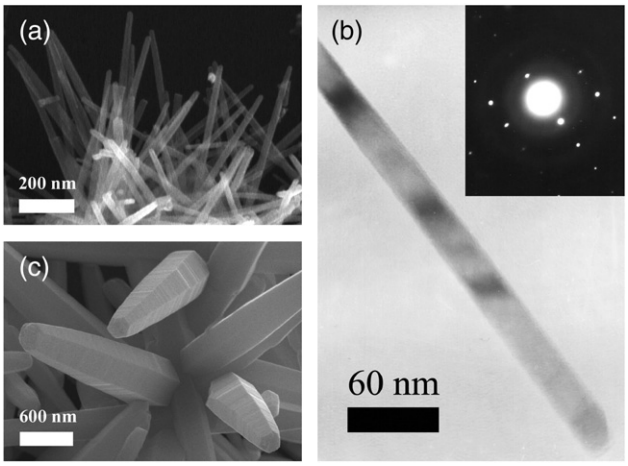

Fig. 1. (a) SEM and (b) TEM images with inset SAED pattern of ZnO nanorods obtained by introducing sols prior to the hydrothermal reaction; (c) SEM image of ZnO nanorods by one-step hydrothermal reaction.

the structural and optical properties of ZnO nanorods are investigated. The influences of the number of seed nuclei and the aging time of ZnO sols on the morphology of ZnO nanorods are also discussed.

2. Experimental

The experimental procedure was carried out in two steps as follows: first, 0.55 g zinc acetic dehydrate and 0.145 g lithium hydroxide monohydrate were respectively dissolved in 30 ml of ethanol and then the solutions were mixed at 50 °C for 5 min to obtain ZnO sols with a diameter of about 3 nm. 1.2 ml colloid solution was directly dropped to 30 ml of the aqueous solution containing 0.025 mol/l zinc nitrate and 0.025 mol/l methenamine in a Teflon-lined autoclave. Second, the autoclave was sealed and heated at 90 °C for 3 h and then cooled to room temperature. The white precipitate in the bottom of the autoclave was collected, centrifugated, washed using deionized water and dried at 60 °C in air.

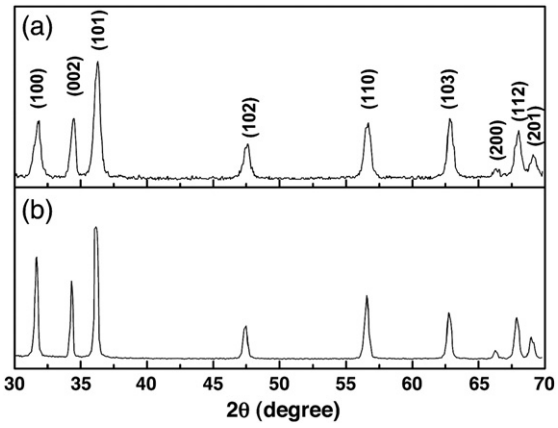

Fig. 2. XRD spectra of ZnO nanorods (a) via two-step reaction and (b) via one-step hydrothermal reaction.

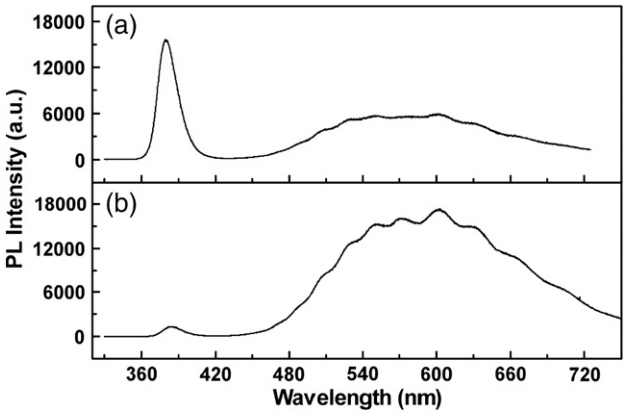

Fig. 3. PL spectra of ZnO nanorods (a) via two-step reaction and (b) via one-step hydrothermal reaction.

The morphology of the ZnO was examined with field-emission scanning electron microscope (FESEM; Hitachi S-4800) and transmission electron microscopy (TEM; JEOL 2010). The structure was analyzed by X-ray diffraction (XRD; Rigaku D/max-rA) and selected area electron diffraction (SAED). A He–Cd laser at 325 nm was used to obtain photoluminescence (PL) spectra and resonant Raman spectra, which were performed using a LABRAM-UV Raman microspectrometer (Jobin Yvon). Optical absorption spectra were investigated with a UV-360 spectrophotometer (Shimadzu).

3. Results and discussion

Fig. 1(a) and (b) shows SEM and TEM images of ZnO nanorods, respectively. For comparison, the SEM image of ZnO nanorods without introducing sols is also given in Fig. 1(c). As shown in Fig. 1(a) and (b), the width of nanorods is about 25 nm, and the length is over 500 nm. The inset of Fig. 1(b) corresponds to the SAED pattern of ZnO nanorods, indicating that the obtained nanorod is single-crystal wurtzite ZnO and oriented in the *c*-axis direction. Clearly, the width of the nanorod decreases at least an order of magnitude and the aspect ratio increases from 4 to 20 when ZnO sols are introduced prior to the hydrothermal process.

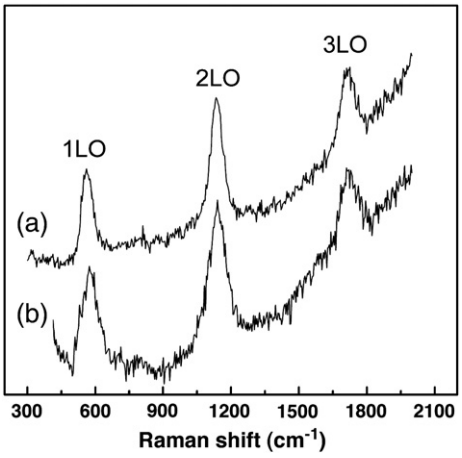

Fig. 4. Resonant Raman spectra of ZnO nanorods (a) via two-step reaction and (b) via one-step hydrothermal reaction.

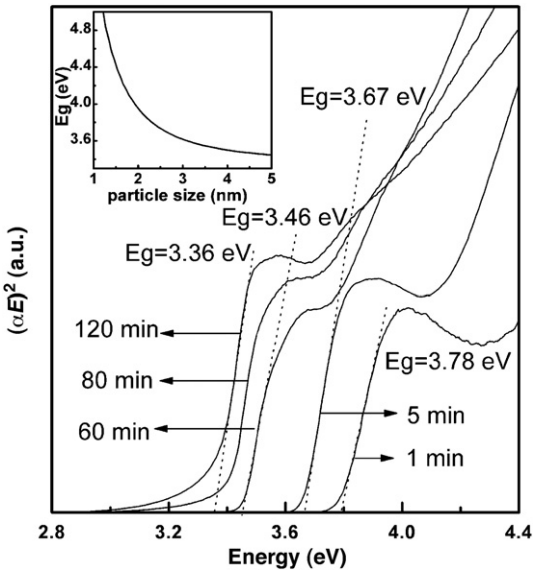

Fig. 5. Plot of $(\alpha E)^2$ versus energy E at different aging times. The inset shows the plot of the band gap energy versus the average particle size according to effective mass approximation.

Fig. 2 shows XRD spectra of ZnO nanorods with and without introducing sols. All diffraction peaks can be indexed to the hexagonal wurtzite ZnO. Compared with the ZnO nanorods without introducing sols, all diffraction peaks of the obtained ZnO nanorods with introducing sols are broadened. The peak broadening can be caused by two possible factors, i.e., the inhomogeneous strains and the decreased size [15]. The inhomogeneous strains also cause the shifts of the diffraction peaks while the size is independent of the peak positions [15]. Since the positions of all diffraction peaks are almost unchanged, as shown in Fig. 2, the influence of inhomogeneous strains on the peak broadening can be ignored. Therefore, compared with the ZnO nanorods without introducing sols, the broadened diffraction peaks for the ZnO nanorods with introducing sols indicate the decreased size, which is in good agreement with the SEM results. From Fig. 2(a), the full width at half maximum (FWHM) of (002) peak is obviously narrower than that of other diffraction peaks. This indicates the oriented growth of the single ZnO nanostructure along the [0001] direction according to the Scherrer formula, which is consistent with the SAED result.

Fig. 3 is the room-temperature PL spectra of the ZnO nanorods grown with and without introducing sols. The typical ZnO PL spectra composed of ultraviolet (UV) emission peak and visible emission band can be observed. The UV peak is due to the exciton recombination while the visible spectral region ranging from 440 to 800 nm is attributed to defect emission related to surfaces [16]. The intensity ratio of UV to visible emissions can be used to evaluate the quality of ZnO [17,18]. Although it is generally assumed that smaller-size ZnO nanostructures correspond to a lower intensity ratio of UV to visible emissions due to larger surface area-to-volume ratio and more surface defects [19–21], a stronger UV emission relative to the visible emission is observed in the smaller-size ZnO nanorods in our experiment. One possible reason is the formation of steps at the side surfaces of the larger-size ZnO nanorods, as shown in Fig. 1c, which may increase the surface/interface defects. Therefore, the increased intensity ratio of ultraviolet to visible emissions shows the improved crystal quality for ZnO nanorods obtained by introducing sols.

Fig. 4 shows resonant Raman spectra of ZnO nanorods fabricated with and without introducing sols. When the samples were excited by the 325 nm line of a He–Cd laser, the incoming photon energy is resonant with the electronic interband transition energy of the wurtzite ZnO. In this case, the incoming resonant will occur. As shown in Fig. 4, an intense multiphonon process with three phonon lines centered at about 563, 1130, and 1710 cm^{-1} is observed in resonant Raman spectra, which originate from A_1(LO) and E_1(LO) modes and their overtones [22]. Compared with the larger-size nanorods, the LO phonons of the smaller-size nanorods shift toward the lower frequency, and their FWHMs decrease. The Raman shifts are most likely caused by the local heating by UV laser excitation. The smaller nanostructures contain more air gaps, and hence possess the smaller thermal conductivity resulting in a low-frequency shift [23]. Generally, the smaller-size nanostructures have a broader size distribution and hence correspond to larger linewidths of Raman peaks. From SEM image, the size distribution of the nanorods obtained by introducing sols is quite narrow. Furthermore, the single nanorod has a uniform width along its entire length. These may result in the narrower Raman linewidths in smaller-size nanorods.

In our experiment, we found that the amount of the sol must be large so that the solute (ZnO) concentration in the solution can be lowered rapidly below the saturated value in the initial stage of the hydrothermal process. When the number of the seed nuclei is large enough to suppress the formation of new crystal nuclei, changing the amount of the introduced sol will not change the size, shape and uniformity of obtained ZnO nanorods. The residual ZnO sols, because of their much smaller size, may be efficiently separated by centrifugation. However, if the amount of the sol decreases to below 0.01 ml, the two kinds of ZnO nanorods with obvious different sizes are simultaneously obtained (not shown here). The width of the smaller nanorods is about 300 nm, and that of the larger is over 800 nm, which may originate from the spontaneous nucleation in solution and heterogeneous nucleation based on the ZnO sols, respectively. On the other hand, we also studied the influence of aging time of the sols on the morphology of ZnO nanorods. The band gap energy of ZnO sols can be determined from the linear part of a plot of $(\alpha E)^2$ versus energy E by the measurement of the absorption spectra, as shown in Fig. 5. According to the effective mass approximation [24], the plot of band gap energy versus the average particle size of sols is given in the inset of Fig. 5. When the aging time is 1 and 5 min, the obtained ZnO nanorods have similar size and shape. This is due to the weak change in the size of the introduced seed nuclei. However, when the aging time increases from 5 to 60 min, corresponding to the increase of the average

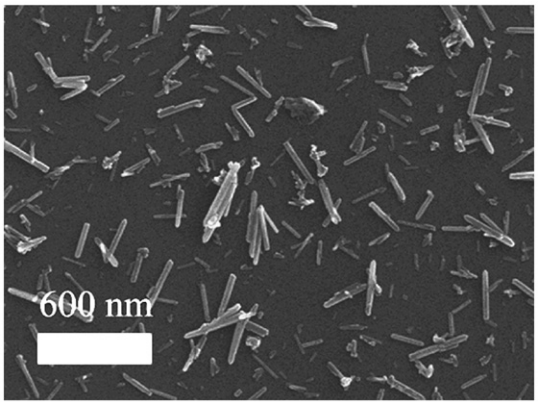

Fig. 6. The product obtained by introducing ZnO sols with the aging time of 60 min prior to hydrothermal reaction.

particle size from 2.7 to 4.7 nm, the obtained nanorods have a fairly broad size distribution with diameters ranging from 20 to 50 nm, and the aspect ratio is decreased to below 10, as shown in Fig. 6. Additionally, some nanoparticles with the diameter of tens of nanometers can be observed, which may be the aggregates of the sols. According to the Ostward ripening, the surface of the aggregate gradually becomes smooth, and the surface defects are decreased during a long aging process in the first-step reaction. As a result, the surface activity is lowered so that the aggregate can not act as nucleation center but independently exists in the second-step hydrothermal process.

4. Conclusions

In summary, we have demonstrated a simple method to synthesize ZnO nanorods of 25 nm with fairly uniform size and shape by introducing ZnO sols prior to hydrothermal reaction. After excessive ZnO sols are introduced, the width of the obtained nanorods decreases above an order of magnitude and the aspect ratio increases 5 times. This synthesis route may be also feasible for the fabrication of other small-size metal oxide nanostructures. For smaller-size ZnO nanorods, PL measurements show the stronger intensity ratio of UV to visible emissions and resonant Raman spectra show narrower Raman lines, which may originate from the uniform width of the single nanorod along its length and the narrow size distribution.

Acknowledgements

This work is supported by the Key Project of the National Natural Science Foundation of China under Grant No. 60336020, the Innovation Project of Chinese Academy of Sciences, the National Natural Science Foundation of China under Grant Nos. 60278031, 60376009, 50402016, 60506014, 60501025 and 60576040, the Cultivation Fund of the Key Scientific and Technical Innovation Project (No. 704017), the State Natural Science Foundation – Outstanding Overseas Chinese Young Scholar Foundation No. 60429403, and the Direct Allocation Grant of Research Grants Committee of Hong Kong, No. DAG04/05.SC24.

References

[1] Y. Xia, P. Yang, Y. Sun, Y. Wu, B. Mayers, B. Gates, Y. Yin, F. Kim, H. Yan, Adv. Mater. 15 (2003) 353.
[2] U. Ozgur, Y.I. Alivov, C. Liu, A. Teke, M.A. Reshchikov, S. Dogan, V. Avrutin, S.-J. Cho, H. Morkoc, J. Appl. Phys. 98 (2005) 041301.
[3] M.H. Huang, S. Mao, H. Feick, H.Q. Yan, Y.Y. Wu, H. Kind, E. Weber, R. Russo, P.D. Yang, Science 292 (2001) 1897.
[4] Z.W. Pan, Z.R. Dai, Z.L. Wang, Science 291 (2001) 1947.
[5] J. Zhang, L.D. Sun, C.S. Liao, C.H. Yan, Chem. Commun. 3 (2002) 262.
[6] B. Liu, H.C. Zeng, J. Am. Chem. Soc. 125 (2003) 4430.
[7] L. Vayssieres, K. Keis, A. Hagfeldt, S. Lindquist, Chem. Mater. 13 (2001) 4395.
[8] L. Vayssieres, K. Keis, S. Lindquist, A. Hagfeldt, J. Phys. Chem., B 105 (2001) 3350.
[9] B. Cheng, E.T. Samulski, Chem. Commun. 8 (2004) 986.
[10] Z. Tian, J.A. Voigt, J. Liu, B. Mckenzie, M.J. Mcdermott, M.A. Rodriguez, H. Konishi, H. Xu, Nat. Mater. 2 (2003) 821.
[11] L.E. Greene, M. Law, J. Goldberger, F. Kim, J.C. Johnson, Y. Zhang, R.J. Saykally, P. Yang, Angew. Chem., Int. Ed. 42 (2003) 3031.
[12] Y. Tseng, C. Huang, H. Cheng, I. Lin, K. Liu, I. Chen, Adv. Funct. Mater. 13 (2003) 811.
[13] Q. Li, V. Kumar, Y. Li, H. Zhang, T.J. Marks, R.P.H. Chang, Chem. Mater. 17 (2005) 1001.
[14] H. Yu, Z. Zhang, M. Han, X. Hao, F. Zhu, J. Am. Chem. Soc. 127 (2005) 2378.
[15] G.Z. Cao, in: G.Z. Cao (Ed.), Nanostructures and Nanomaterials: Synthesis, Properties, and Applications, Imperial College Press, London, 2004, p. 331.
[16] Y.H. Tong, Y.C. Liu, C.L. Shao, R.X. Mu, Appl. Phys. Lett. 88 (2006) 123111.
[17] M. Izaki, T. Shinagawa, H. Takahashi, J. Phys., D, Appl. Phys. 39 (2006) 1481.
[18] M. Izaki, S. Watase, H. Takahashi, Appl. Phys. Lett. 83 (2003) 4930.
[19] B.D. Yao, Y.F. Chan, N. Wang, Appl. Phys. Lett. 81 (2002) 757.
[20] M.H. Huang, Y.Y. Wu, H. Feick, N. Tran, E. Weber, P.D. Yang, Adv. Mater. 13 (2001) 113.
[21] Q. Tang, W. Zhou, J. Shen, W. Zhang, L. Kong, Y. Qian, Chem. Commun. 6 (2004) 712.
[22] H.M. Cheng, H.C. Hsu, Y.K. Tseng, L.J. Lin, W.F. Hsieh, J. Phys. Chem., B 109 (2005) 8749.
[23] H. Cheng, K. Lin, H. Hsu, C. Lin, L. Lin, W. Hsieh, J. Phys. Chem., B 109 (2005) 18385.
[24] Z.Y. Xiao, Y.C. Liu, L. Dong, C.L. Shao, J.Y. Zhang, Y.M. Lu, D.Z. Zhen, X.W. Fan, J. Colloid Interface Sci. 282 (2005) 403.